Elsevier Editorial System(tm) for Journal of Hazardous Materials

Manuscript Draft

Manuscript Number: HAZMAT-D-20-00523

Title: Probing the synthetic P-type zeolite to the efficient removal of heavy metal from aqueous solution

Article Type: Research Paper

Keywords: heavy metal; zeolite; uptake capacity; high efficiency.

Corresponding Author: Professor fuqiang huang,

Corresponding Author's Institution: Shanghai Institute of Ceramics,Chinese Academy of Sciences

First Author: Mingyue Chen

Order of Authors: Mingyue Chen; Shuying Nong; Yantao Zhao; Muhammad Sohail Riaz; Yi Xiao; Maxim S Molokeev; fuqiang huang

Abstract: Zeolite is a characteristic material for removing heavy metals exhibiting by low tolerance quantities. It is particularly desirable although challenging to cultivate an unmodified and reusable zeolite for eradicating heavy metals with great capacity. Herein, we sought out and firstly synthesized the uniform octahedral zeolite $Na_6Al_6Si_{10}O_{32}\cdot 12H_2O$ for heavy metal ions trap, proven extraordinarily effective decontamination of M^{2+} (M = Pb, Cd, Cu, and Zn). The maximum capacities of Pb^{2+}, Cd^{2+}, Cu^{2+}, and Zn^{2+} were 649, 210, 90 and 88 mg/g, and the distribution coefficients (Kd) was~108 mL/g for Pb^{2+} which emphasized the superior effectiveness of $Na_6Al_6Si_{10}O_{32}\cdot 12H_2O$ contrasted with other zeolites. Rapid adsorption was observed that Pb^{2+} concentration (7.5 ppm) was reduced to 0.6 ppb in 2 min. The removal mechanism was ascribed to the ion exchange and the hydroxyl groups thereby affording high adsorption capacity. We also investigated the heavy metal removal of zeolite 13X and 4A for comparison and concluded the determining factor affecting absorption capacity. The removal rate of Pb remained at 97.4% even after five regeneration recycles. The zeolite was therefore promising for practical water purification and industrialization.

Suggested Reviewers: Mercouri G Kanatzidis
m-kanatzidis@northwestenrn.edu
He is an expert on this topic.

Dear Editor,

We would like to submit the enclosed manuscript entitled “Probing the synthetic P-type zeolite to the efficient removal of heavy metal from aqueous solution” for publication as article in *Journal of Hazardous Materials*.

Heavy metal contamination is a core environmental issue threatening human health and the adsorption technology is sustainable and economical for heavy metal removal. Zeolite is characteristic absorption material for removing heavy metal contributed to easily attained, recycling and less secondary pollution. To achieve further heavy metal adsorption capacity, surface functionalization and designing composites for zeolite are successfully performed. However, the tolerance quantities are not comparable with other absorbents and the preparation process is complicated. Importantly, many researches about zeolites do not provide the residual concentration of heavy metal after absorption and it is not sure the removal efficiency. Therefore, it is particularly desirable to develop an unmodified zeolite for eradicating heavy metal with great capacity.

In this work, we sought out and firstly synthesized uniform octahedral zeolite $Na_6Al_6Si_{10}O_{32}\cdot 12H_2O$ without modification for purifying heavy metal to drinkable level. The maximum capacities of Pb^{2+}, Cd^{2+}, Cu^{2+}, and Zn^{2+} were 649, 210, 90 and 88 mg/g that were comparable with other absorbents and the reason why adsorbent affinity followed the order Pb>Cd>Cu>Zn was discussed. Rapid adsorption was observed that Pb^{2+} concentration (7.5 ppm) could be reduced to 0.6 ppb in 2 min emphasized the superior effectiveness of $Na_6Al_6Si_{10}O_{32}\cdot 12H_2O$. The ion exchange and the hydroxyl groups afforded the excellent performance. We also investigated the heavy metal removal of zeolite 13X and 4A for comparison and concluded the determining factor affecting absorption capacity: (1) phase purity, (2) cation exchange capacity, (3) pore size on the zeolite framework, (4) the OH groups of zeolites. The reusable zeolite that removal rate of Pb remained at 97.4% even after five regeneration recycles was therefore promising for practical water purification and industrialization.

The Journal of Hazardous Materials focuses on the environmental relevance and significance of the studied materials. In our study, we firstly prepared the pure zeolite $Na_6Al_6Si_{10}O_{32}\cdot 12H_2O$ with uniform octahedral shape used for environmental remediation and investigated the property of eradicating heavy metal in detail. According to the comparison of other zeolites, we proposed and verified the insights impacting the absorption capacity of zeolites. We believe our work is important and timely, and hence it will be of great interest to the readers of Journal of Hazardous Materials.

Thank you for your consideration.

Sincerely,

Prof. Fuqiang Huang

E-mail: huangfq@pku.edu.cn

Beijing National Laboratory for Molecular Sciences and State Key Laboratory of Rare Earth Materials Chemistry and Applications, College of Chemistry and Molecular Engineering, Peking University, Beijing 100871, China

*Novelty Statement (maximum limit:100 words)

Statement of novelty

This work firstly prepared the pure zeolite $Na_6Al_6Si_{10}O_{32}\cdot 12H_2O$ with uniform octahedral shape through regulating the ratio of Al/Si/NaOH/H_2O and investigated the property for eradicating heavy metal detailedly. The results proved the higher absorption capacities and faster absorption rates than other zeolites. It also explained the relationship between adsorbent affinity and physicochemical properties of the heavy metals. The performance of heavy metal removal of other zeolites was studied for comparison and we proposed and verified the insights impacting the absorption capacity of zeolites. Our work focused on the environmental relevance and significance of the materials, suited to Journal of Hazardous Materials.

Probing the synthetic P-type zeolite to the efficient removal of heavy metal from aqueous solution

Mingyue Chen[†], Shuying Nong[†], Yantao Zhao[†], Muhammad Sohail Riaz[†], Yi Xiao[†], Maxim S Molokeev[Δ,⊥] and Fuqiang Huang[*,†,§]

[†] Beijing National Laboratory for Molecular Sciences and State Key Laboratory of Rare Earth Materials Chemistry and Applications, College of Chemistry and Molecular Engineering, Peking University, Beijing 100871, China

[Δ] Siberian Federal University, Krasnoyarsk, 660041, Russia

[⊥] Department of Physics, Far Eastern State Transport University, Khabarovsk, 680021 Russia

[§] CAS Key Laboratory of Materials for Energy Conversion and State Key Laboratory of High-Performance Ceramics and Superfine Microstructure, Shanghai Institute of Ceramics, Chinese Academy of Sciences, Shanghai 200050, P. R. China

* Corresponding author: Prof. Fuqiang Huang

E-mail address: huangfq@pku.edu.cn

ABSTRACT

Zeolite is a characteristic material for removing heavy metals exhibiting by low tolerance quantities. It is particularly desirable although challenging to cultivate an unmodified and reusable zeolite for eradicating heavy metals with great capacity. Herein, we sought out and firstly synthesized the uniform octahedral zeolite $Na_6Al_6Si_{10}O_{32}\cdot 12H_2O$ for heavy metal ions trap, proven extraordinarily effective decontamination of M^{2+} (M = Pb, Cd, Cu, and Zn). The maximum capacities of Pb^{2+}, Cd^{2+}, Cu^{2+}, and Zn^{2+} were 649, 210, 90 and 88 mg/g, and the distribution coefficients (K_d) was$\sim 10^8$ mL/g for Pb^{2+} which emphasized the superior effectiveness of $Na_6Al_6Si_{10}O_{32}\cdot 12H_2O$ contrasted with other zeolites. Rapid adsorption was observed that Pb^{2+} concentration (7.5 ppm) was reduced to 0.6 ppb in 2 min. The removal mechanism was ascribed to the ion exchange and the hydroxyl groups thereby affording high adsorption capacity. We also investigated the heavy metal removal of zeolite 13X and 4A for comparison and concluded the determining factor affecting absorption capacity. The removal rate of Pb remained at 97.4% even after five regeneration recycles. The zeolite was therefore promising for practical water purification and industrialization.

Key words: heavy metal; zeolite; uptake capacity; high efficiency

1. Introduction

Heavy metal contamination, derived from batteries, electronics, electroplating, tanneries, petrochemicals, is becoming a core issue in environmental remediation due to toxicity and non-biodegradable, threatening human health via the entire food chain [1, 2]. The adsorption in terms of high removal efficiency, renewable, environmentally friendly and the flexibility in design and operation is considered to be a sustainable and economical technology for heavy metal removal. Until now, various adsorbents have been established for investigating removal performance and the adsorption mechanism of which mainly depended on ion exchange, complexation, and electrostatic attraction. Contemplating that complexation and electrostatic attraction are dominated by a surface-based process, many efforts should be devoted to the synthesis of absorbents with preferred structure and functionalized with complex groups[3-6]. The layered double hydroxides (LDHs) functionalized with polysulfide $[S_x]^{2-}$ and MoS_4^{2-} anions improve metal uptake capacity owing to the interaction between heavy metal cations and sulfide anions[7, 8]. These absorbents are hard to prepare and inadequate for industrialization. Conversely, ion exchange is the reversible exchange of ions between the liquid phase and solid phase without any radical change of solid structure, which is widely utilized industrial technique in wastewater treatment as well as separation process due to reasonable cost and process simplicity. Diverse ion-exchange adsorbents, such as layered sulfides, zeolite[9], resin[10], clay[11, 12], are established for water treatment. The layered sulfides $K_xBi_{4-x}Mn_xS_6$, $K_{2x}Mn_xSn_{3-x}S_6$, $K_{2x}Sn_{4-x}S_{8-x}$ and $K_{0.48}Mn_{0.76}PS_3{\cdot}H_2O$ demonstrate excellent removal efficacy of heavy metals through ion-exchange[13-16]. The exchange capacity of $K_xBi_{4-x}Mn_xS_6$ for Cd^{2+} and Pb^{2+} are 221 and 342 mg/g respectively and the K_d is $\sim 10^7$ mL/g. Unfortunately, the constancy and cycle property of sulfides is not impressive. Clay is a low-cost adsorbent, but they suffer from a weak affinity for heavy metals. Even though the ion exchange resin is a common absorbent for practical application, it will lead to secondary pollution.

Amongst ion-exchange absorbents, zeolites are microporous crystalline aluminosilicates that are well known for its uniform channels and cavities, which is especially suitable for water treatment contributed to easily attained, recycling and less secondary pollution[17]. Notably, they are low cost and accessible in bulk. The adsorption capacities of natural zeolites for Pb^{2+}, As^{5+}, Cu^{2+}, Zn^{2+} and Ni^{2+} are 125.2, 20.31, 14.65, 13.54 and 11.68 mg/g respectively[18]. An interesting class of materials

for the environmental remediation is the modified zeolites, which enhances sorption capacity by introducing complex functional groups[19, 20]. Besides, the synthesized zeolite has a bigger cation exchange capacity (abbreviate as CEC) than natural zeolite due to no impurities in the ion exchangers and hence the uptake capacities of synthesized zeolite NaX for Pb^{2+} and Cu^{2+} are better.[21, 22] Despite these signs of progress, to the best of our knowledge, the existing zeolites still suffer from low sorption capacity and removal effectiveness compared to other absorbents.

Herein, we seek out a zeolite $Na_6Al_6Si_{10}O_{32}\cdot 12H_2O$ (abbreviate as NASO) and successfully prepare the pure phase using hydrothermal method through regulating the ratio of Al/Si/NaOH/H_2O, which is adept for water treatment. The synthesized NASO without any modification manifest highly effective decontamination of heavy metal ions M^{2+} (M = Pb, Cd, Cu, and Zn) from aqueous media and the maximum capacities of Pb^{2+}, Cd^{2+}, Cu^{2+} and Zn^{2+} are 649, 210, 90 and 88 mg/g which is much better than other zeolites. The NASO can diminish Pb^{2+}concentration down to < 1 ppb at the low or massive concentration (4 and 130 ppm) and the K_d reached to $\sim 10^8$ mL/g. The removal rate of NASO for Pb^{2+} (200 ppm) still kept at 97.4% after 5 cycles, which proved the NASO was a top material known for the rapid separation of pollutants. Significantly, the low cost and easy preparation make the NASO be suitable for industrialization.

2. Materials and methods

2.1 Preparation of NASO ($Na_6Al_6Si_{10}O_{32}\cdot 12H_2O$)

All the chemicals used in the experiments were of analytical grade and used without further purification. NASO was synthesized using a facile hydrothermal method. Simply, solution A was prepared by dissolving $Al(NO_3)_3\cdot 9H_2O$ (0.45 g) in 10 mL deionized water. Solution B was got by dissolving $Na_2SiO_3\cdot 9H_2O$ (0.68 g) in 10 mL deionized water. The mixed solutions were prepared through the addition of solution B into solution A to form a homogeneous solution with vigorously magnetic stirring for 10 min. Subsequently, NaOH solution (0.23 g NaOH dissolving in 10 mL deionized water) was quickly added, and after 10 min further stirring the resultant solution was sealed in Teflon-lined stainless autoclave (50 ml). The autoclave was heated to 160 ^oC, kept for 24 h, and then samples were cooled to room temperature naturally. After that, the solid material was separated by centrifuging and sequentially washed with deionized water several times to remove the basic solution and then dried at 80 °C for 2 h.

2.2 Batch absorption experiments

The absorption experiments of heavy metal M^{2+} ions (M = Pb, Cd, Cu, and Zn) were performed at ambient temperature using the NASO material at the pH values of 3-5 (natural pH values and adjusted with the aid of 1 wt% HNO_3 solution). The individual heavy metal solution under various initial concentrations (5-1000 ppm) was prepared by dissolving $Pb(NO_3)_2$, $Cd(NO_3)_2$, $Cu(NO_3)_2$ and $Zn(NO_3)_2$ in deionized water respectively. All batch experiments were conducted through dispersing 0.01 g NASO into 10 mL aqueous solutions (V:m = 1000 mL/g) under stirring. The NASO particles were separated by a 0.2 μm nylon filter membrane and the residual solutions were taken to further analysis. The adsorption isotherms were established by adding NASO materials to the solution containing individual M^{2+} ions with various initial concentrations (5-1000 ppm) stirred for 24 h. The pH values of low M^{2+} concentration was 5 adjusted by 1 wt% HNO_3 solution and the pH values of heavy M^{2+} concentration was the natural pH about 3-4. Adsorption kinetic experiments for heavy metal M^{2+} ions under different contact time (2-240 min) were conducted.

One measure of a sorbent's affinity for a target metal ion is the distribution coefficient (K_d) measurement[23]. The K_d was the ratio of the amount of M^{2+} ions adsorbed by one gram of the sorbent to that remaining in solution calculated via the equation (1):

$$K_d = \frac{V(C_0 - C_e)/C_e}{m} \qquad (1)$$

The removal capacity (q_e) was given by the equation (2):

$$q_e = \frac{V(C_0 - C_e)\times 10^{-3}}{m} \qquad (2)$$

The removal % was obtained from the equation (3):

$$\text{Removal \%} = \frac{(C_0 - C_e)\times 100}{C_0} \qquad (3)$$

where C_0 and C_e were the initial and equilibrium concentrations of heavy metal ions (ppm) after the absorption, respectively; V is the solution volume (L) and m is the adsorbent mass (g).

2.3 Characterization

Powder X-ray diffraction (XRD) measurements were performed on a Bruker D2 phaser diffractometer, operating at 40 kV and 100 mA with Cu Ka radiation (λ = 1.5406 Å). The scanning rate for phase identification was fixed at 5° min^{-1} with a 2θ

range from 10° to 60°. The scanning electron microscopy (SEM) images and energy dispersive X-ray spectroscopy (EDS) analyses were attained by a Hitachi S-4800 field-emission electron microscope. The zeta potential of sorbent was measured using a zeta plus (Brookhaven, USA) at various pH from 3 to 6. The X-ray photoelectron spectros-copy (XPS) was performed by an Axis Ultra Photoelectron Spec-trometer (Kratos Analytical Ltd.) using a monochromatized Al Kα anode (225 W, 15 mA, and 15 kV). The C 1s peak at 284.8 eV was taken as an internal standard. The FTIR spectrum were recorded within the range 400-4000 cm^{-1} using an FTIR spectrophotometer (IR-Prestige 21, Shimadzu, Japan) with KBr as the matrix.

The M^{2+} ions concentration in the range of 1-100 ppm before and after absorption were measured through a Leeman Prodigy 7 spectrometer inductively coupled plasma-atomic emission spectroscopy (ICP-OES). Standards of these ions were prepared by diluting the commercial ~1000 ppm ICP standards, and the calibration was liner with maximum errors of 5%. The equilibrium concentrations of M^{2+} ions in the solutions for extra low concentration (at ppb level) were determined by inductively coupled plasma-mass spectroscopy (ICP-MS) using a PerkinElmer NexION 350X ICP-MS spectrometer.

3. Results and discussion

3.1 Structural analysis of NASO and heavy metal removal

The structure of NASO was, shown in Figure 1(a), a three-dimensional framework built from corner sharing SiO_4 and AlO_4 tetrahedra linked through oxygen atoms and the dominated channel size was 8.8 Å. The isomorphous replacement of Si^{4+} by Al^{3+} produced negative charges in the lattice balanced via the exchangeable Na ions which were located at the channels. The XRD pattern and SEM image of NASO were depicted in Figure 1(b) and Figure 1S. It could be observed that all peaks were assigned to the $Na_6Al_6Si_{10}O_{32}{\cdot}12H_2O$ (JCPDS card no. 71-0962) without forming any impurity phase and the NASO crystallizes in the tetragonal space group I-4 with a = 10.043 Å, c = 10.043 Å, V = 1012.96 $Å^3$. The morphology of NASO was characterized as a uniform octahedral with clear crystal edges which confirmed that it was well crystallized in the range of 12-20 μm. The uptake of heavy metal ions by NASO from solution in the same concentration (10 ppm) was conducted to explore whether it can be used for the removal of heavy metal ions. The results of SEM and EDS mapping suggested that the NASO owned the ability to adsorb heavy metal M^{2+} (M = Pb, Cd, Cu, and Zn) as elucidated in Figure 1(c). Nevertheless, the octahedron

was cracked referred as the introduction of heavy metals. Finally, the XRD patterns after the adsorption M^{2+} were presented in Figure 1(a) indicating no impurity phase.

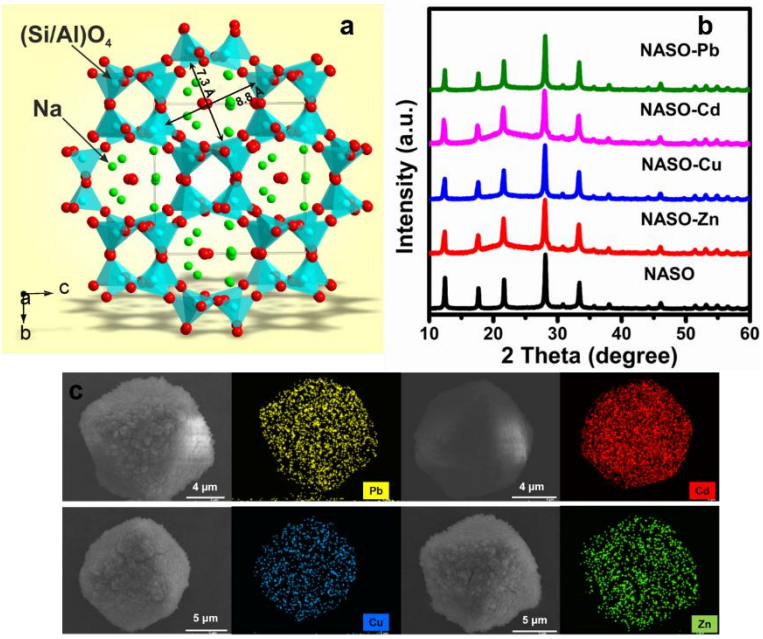

Figure 1. (a) The crystal structure of NASO; (b) XRD patterns of NASO before and after adsorption of 10 ppm M^{2+}; (c) SEM images and EDS mapping for the NASO after adsorption of M^{2+} with 10 ppm concentration.

3.2 Effect of initial pH

Solution pH, one key factor that affected the sorption of heavy metals significantly, determined the metal speciation and surface charge of the adsorbent[24]. Therefore, the Pb^{2+} removal rates of different initial concentration as a function of pH (3.0-6.0) were carried out in batch. At this pH range, precipitation was not the dominant process. From Figure 2(a), it was apparent that the Pb^{2+} sorption results were favored at larger pH values. The results were in agreement with the changing of zeta potential of NASO, which NASO charges became more negative at higher pH owing to the ionization of Si-OH and Al-OH groups shown in Figure 2(b)[25]. The main Pb^{2+} species were presented as Pb^{2+}, $Pb(OH)^{+}$ in the pH range of 2-6 at 25 ^{o}C[26]. The Pb^{2+} ions predominate in solution at pH $\leq$ 5, the competition from H^{+} decreased the Pb^{2+} removal via ion exchange and the NASO could be dissolved slightly under low pH 2-3[27, 28]. Meanwhile, the more negative charges on the surface of NASO enhanced removal capacity at a bigger pH (Figure 2(a)). However, for pH= 6, the presence and adsorption of $Pb(OH)^{+}$ might prevent Pb^{2+} diffusion to some sites within the porous structure[29]. Hence, the pH value was kept at 5.0, which was the same for Cd^{2+}, Cu^{2+}, and Zn^{2+}.

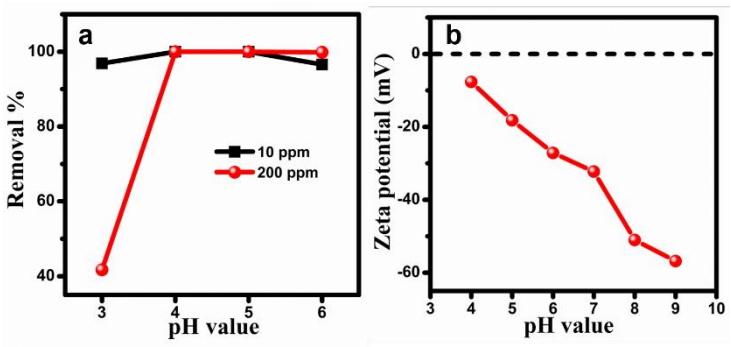

Figure 2. (a) Effect of initial pH value on removal rates of different Pb^{2+} concentrations (10 and 200 ppm) by NASO; (b) zeta potential measurement plots of NASO at different pH values.

3.3 Sorption isotherm toward M^{2+} and removal capacity

Based on the above results, the NASO disclosed acceptable sorption for M^{2+} (M = Pb, Cd, Cu, and Zn). The batch sorption experiments at ambient temperature within a wide range of M^{2+} concentrations were conducted. The initial and residual concentrations of M^{2+} in the aqueous solution could be acquired through ICP measurements. As shown in Table 1 and Table S1, the M^{2+} ions captured by NASO increased significantly with the increasing of initial concentrations. On a broad range of initial concentration (4-400 ppm), the Pb^{2+} removal rates reached >99.9% and the K_d values ranged from 1.74 $\times 10^6$ to 5.15 $\times$ 10^8 mL/g. The K_d represents the performance metrics of metal ion removal for any sorbent, and K_d values of 1.0 $\times$ 10^5 mL/g are considered excellent[3, 30]. The removal rates of Cd^{2+} were > 99.95% with the initial concentration of 10-100 ppm and the corresponding K_d values were about 10^6-10^7 mL/g. For Cu^{2+}, the removal rates were > 99.83% ($K_d \approx 10^5$-10^6 mL/g) in a small range of 10-60 ppm. For Zn^{2+}, the removal rates were relatively lower at >99.47% ($K_d \approx 10^5$ mL/g) with the initial concentration of 5-50 ppm.

The uptake capacity of NASO, another significant aspect of sorbent's performance metric, was calculated by Langmuir and Freundlich isotherms which were expressed as following (4-5):

$$\frac{C_e}{q_e} = \frac{1}{q_{max} K_L} + \frac{C_e}{q_{max}} \qquad (4)$$

$$\ln q_e = \ln K_F + \frac{1}{n} \ln C_e \qquad (5)$$

where q_e (mg/g) is the amount of the heavy metal absorbed at equilibrium concentration, C_e (mg/L) is the equilibrium concentration, q_{max} is the maximum

theoretical sorption capacity of the adsorbent, K_L (L/mg) and K_F (mg/g (mg/L)$^{-1/n}$) represent the Langmuir and Freundlich constants, respectively.

Table 1. Adsorption isotherm data of NASO toward to Pb^{2+} ions.

C_0 (mg/L)	C_e (mg/L)	K_d (ml/g)	q_e (mg/g)	Removal (%)
3.9	0.00007	5.57×10^7	3.90	100
10.3	0.00002	5.15×10^8	10.30	100
40.8	0.0003	1.36×10^8	40.80	100
85.5	0.0004	2.14×10^8	85.50	100
131.2	0.0009	1.46×10^8	131.20	100
203.3	0.0077	2.64×10^7	203.29	99.99
400.4	0.2297	1.74×10^6	400.17	99.94
437.9	1.5886	2.75×10^5	436.31	99.64
603.3	38.402	1.47×10^4	564.90	93.63
799.0	147.664	4.41×10^3	651.34	81.52

m = 0.01 g, V = 10 mL, V:m = 1000 mL/g, Contact time: 24 h

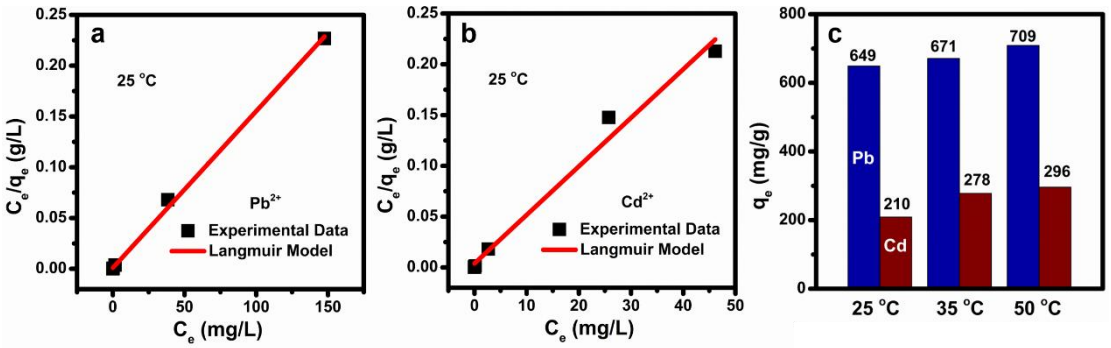

Figure 3. Sorption isotherms for adsorption of (a) Pb^{2+} and (b) Cd^{2+} by NASO; (c) The maximum capacities for Pb^{2+} and Cd^{2+} at different temperatures.

The adsorption isotherms of M^{2+} on NASO were interpreted in Figure 3 and S2, and all the sorption parameters were concluded by the two isotherm equations presented in Table 2. The maximum Pb^{2+} removal capacity reached ~649 mg/g and the correlation coefficient yielded to 0.998. The Langmuir isotherm model better described the equilibrium data, which implied that the adsorption of M^{2+} on NASO was typical monomolecular-layer adsorption with homogeneous binding sites. We also picked up the adsorption capacity of the NASO material for Cd^{2+}, Cu^{2+} and Zn^{2+} and found that the NASO had a maximum adsorption capacity ~210 mg/g for Cd^{2+}. The maximum adsorption capacities for Cu^{2+} and Zn^{2+} were relatively lower at 90 mg/g and 88 mg/g respectively. The uptake capacities of Pb^{2+} and Cd^{2+} could be enhanced by increasing the operation temperature viewed in Figure 3(c) which was

attributed to the bigger kinetic energy of cations at elevated temperature[31]. This was comparable for the other adsorbents as given in Table S2.

Table 2. Adsorption isotherm data of NASO toward to Pb^{2+} and Cd^{2+} ions.

Temperature	25 °C		35 °C		50 °C	
	Pb^{2+}	Cd^{2+}	Pb^{2+}	Cd^{2+}	Pb^{2+}	Cd^{2+}
Langmuir						
q_{max} (mg/g)	649.4	209.2	671.1	277.8	709.2	295.8
K_L (L/mg)	0.9006	1.2225	0.2321	0.1439	0.2242	0.1556
R^2	0.9980	0.9825	0.9916	0.9414	0.9935	0.9643
Freundlich						
K_F ($mg^{1-n}L^n/g$)	378.9	100.8	198.9	48.8	131.9	53.4
1/n	0.1288	0.2497	0.2599	0.3884	0.3564	0.3858
R^2	0.9315	0.8393	0.8337	0.9369	0.7249	0.8407

The analysis of the uptake capacities of four metals at the same condition disclosed that adsorbent affinity followed the order Pb>Cd>Cu>Zn, which was assigned to the physicochemical properties of the heavy metals including electronegativity, hydration radius, first hydrolysis constant and hydration enthalpy[21]. The difference in hydration radius of metals ions was one factor in the ion exchange process, the lower hydration radius of Pb (Pb<Cu<Cd<Zn), presented in Table 3, could pass readily through the channels (8.8 Å) resulting in the biggest capacity. The larger hydration enthalpy (ΔH_{H2O}) of metals (Pb>Cd>Cu>Zn) would boost the adsorption capacity[32]. This was exactly what was observed in this study. The first hydrolysis constants could also be evidence for sorption ability and the higher $\log K_{MOH}$ value exhibited greater sorption capacity[33]. The $\log K_{MOH}$ values for four metals were Pb>Cu>Zn>Cd listed in Table 3. Likewise, the Pauling electronegativity values followed as Pb>Cu>Cd>Zn reflecting the Pb possessed the greatest ionic potential[21]. Hence the Pb had the strongest attraction to the NASO and the sorption ability was Pb>Cu>Zn, which was consistent with the experimental results of sorption capacity. The abnormal Cd sorption capacity might be dominated by the hydration enthalpy that was greater than Cu and Zn.

Table 3. The physicochemical parameters towards Pb, Cd, Cu and Zn.

Metal	Hydrated ionic radius (Å)[34]	Electron-egativity	Hydration enthalpy (ΔH_{H2O} KJ/mol)	Hydrolysis constant $\log K_{MOH+}$[33]
Pb	4.01	2.33	-1479.9[35]	-7.71
Cd	4.26	1.69	-1807[36]	-10.8
Cu	4.19	1.90	-2009[35]	-8.00
Zn	4.30	1.65	-2046[36]	-8.96

3.4 Adsorption kinetics study

The efficiency of NASO for heavy metal removal from aqueous solutions had

been examined by studying the adsorption kinetics. The influence of contact time of M^{2+} ions with NASO was explored to determine adsorption rates and equilibrium times. As depicted in Table 4, Table S3 and Figure 4(a), the adsorption rate for 7.5 ppm Pb^{2+} was especially fast and the residual concentration could be limited to 0.6 ppb within 2 min, the removal rate reached to 99.99% and K_d value was 10^7 mL/g. Nevertheless, the 170 ppm Pb^{2+} could be eliminated to 4.313 ppm within 5 min and the adsorption equilibrium was acquired within 12 h. The ion exchange of zeolite occurred over two distinct stages: fast adsorption on the surface and diffusion in the interior of zeolite.[37] Consequently, the 7.5 ppm Pb^{2+} was adsorbed quickly on the surface of NASO. With the increasing of Pb^{2+} concentration, the absorption rate was fast during the early stage owing to many active sites. Then it took more time to achieve adsorption equilibrium which might be due to the following reasons: (1) the lower Pb^{2+} concentration at the final stage reduced the driving force for ion exchange between NASO and Pb^{2+}, (2) the Pb^{2+} diffusion in the interior took longer time. The capture rate for Cd^{2+} was a little lower than Pb^{2+} under the same experimental conditions, the residual concentration and removal rate was up to 6 ppb (K_d = 10^5 mL/g) and 99.5% within 30 min respectively. The removal rate of Cu^{2+} achieved 99.5% within 60 min, but the subsequent capture became slower and needed more time to reach equilibrium. For Zn^{2+} ions, the removal rate was slow but still 98.5% in 120 min.

Generally, the adsorption rates were determined via Pseudo-first-order and pseudo-second-order models to reveal adsorption behaviors based on the experimental data. The two kinetic rate equations were as follows:

Pseudo-first-order (6):

$$\ln(q_e - q_t) = \ln q_e - k_1 t \qquad (6)$$

Pseudo-second-order (7):

$$\frac{t}{q_t} = \frac{1}{k_2 q_e^2} + \frac{t}{q_e} \qquad (7)$$

where q_e (mg/g) is the amount of heavy metal absorbed at equilibrium concentration, and q_t (mg/g) is the amount of heavy metal adsorbed at time t, while k_1 (min^{-1}) and k_2 (g/mg min^{-1}) are the pseudo-first-order and pseudo-second-order adsorption rate constants respectively. From Figure 4(b), it was observed that the plots of t/q_t vs t of the kinetics data toward four ions Pb^{2+}, Cd^{2+}, Cu^{2+}, and Zn^{2+} exhibited perfect linear relations with high correlation coefficients R^2 closed to 1. The calculated removal

capacities (q_e,cal) of Pb^{2+}, Cd^{2+}, and Cu^{2+} received from the pseudo-second order model were closer to the corresponding experimental values (q_e,exp) as summarized in Table S4. The results indicated all data could be well described via the pseudo-second-order kinetic model, signifying that the M^{2+} removal was chemical adsorption.

Table 4. Kinetics data of Pb^{2+} adsorption using NASO.

C_0 (mg/L)	Time (min)	C_e (mg/L)	K_d (ml/g)	q_t (mg/g)	t/qt (min•g/mg)
7.5	2	0.0006	1.25×10^7	7.499	99.99
	5	0.0009	8.33×10^6	7.499	99.98
	10	0.0005	1.50×10^7	7.500	99.99
	30	0.0006	1.25×10^7	7.499	99.99

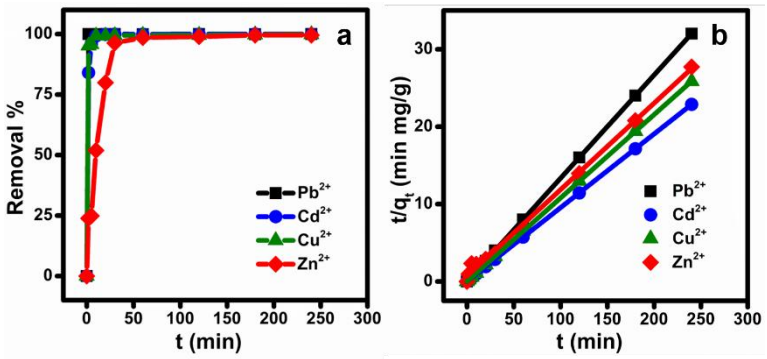

Figure 4. Adsorption kinetics curves for Pb^{2+}, Cd^{2+}, Cu^{2+}, and Zn^{2+}: (a) removal % as a function of contact time; (b) pseudo-second-order kinetic plots for ion adsorption.

3.5 Absorption mechanism

As stated, the amount of Na^+ ions in 1 g $Na_6Al_6Si_{10}O_{32}\cdot 12H_2O$ is 4.59 mmol. To keep the charge balance, the ion exchange equation was $2Na^+ \rightarrow Pb^{2+}$, Hence the theoretical maximum exchange amount of Pb^{2+} ions will be 2.29 mmol. However, the maximum removal capacity of Pb^{2+} is 3.14 mmol (649 mg/g). According to ICP analysis, the amount of Na in 0.01 g NASO was 0.0441mmol and the residual amount of Na in NASO absorbed by 200 ppm Pb^{2+} was 0.0202 mmol. Accordingly, we supposed that there were two components of Pb^{2+} adsorption: (1) Pb^{2+} ions were exchanged by Na^+ ions; (2) Pb^{2+} reacted with the OH groups of the NASO. To better understand the adsorption mechanism, the infrared spectrum (400-4000 cm^{-1}) and XPS analysis of NASO samples before and after Pb^{2+} adsorption were executed presented in Figure 5. As illustrated in Figure 5(a)(b), two peaks appeared at 139.6 eV and 144.3 eV assigned to Pb $4f_{7/2}$ and Pb $4f_{5/2}$ respectively, which advocated that Pb^{2+} was successfully adsorbed on NASO. Additionally, the intensity of peak at 1071 eV

(Na 1s) decreased after Pb^{2+} adsorption, indicating that Na^{+} ions were exchanged by Pb^{2+} (Figure S3). In the FTIR spectra (Figure 5(c)), the bands at 446 cm^{-1}, 929 cm^{-1} and 742 cm^{-1} were corresponding to the bending vibration of $Si(Al)O_4$ tetrahedra, symmetric stretching vibrations of Si-O-Si or Si-O-Al bridges and Al-OH bending vibration, respectively[21]. The strong vibration at 1006 cm^{-1} was correlated with Si(Al)-O asymmetric stretching[38]. The characteristic peaks at 1658 cm^{-1} and 3476 cm^{-1} was associated with the bending vibration of -OH belonging to the water molecule[17]. After Pb^{2+} absorption, the intensities of peaks at 929 cm^{-1}, 1658 cm^{-1} and 3476 cm^{-1} reduced originated from the Pb-O vibrations, confirming the involvement of hydroxyl groups in the Pb^{2+} removal process. The above results proved the proposed absorption mechanism and the schematic diagram of the adsorption mechanism was given in Figure 6.

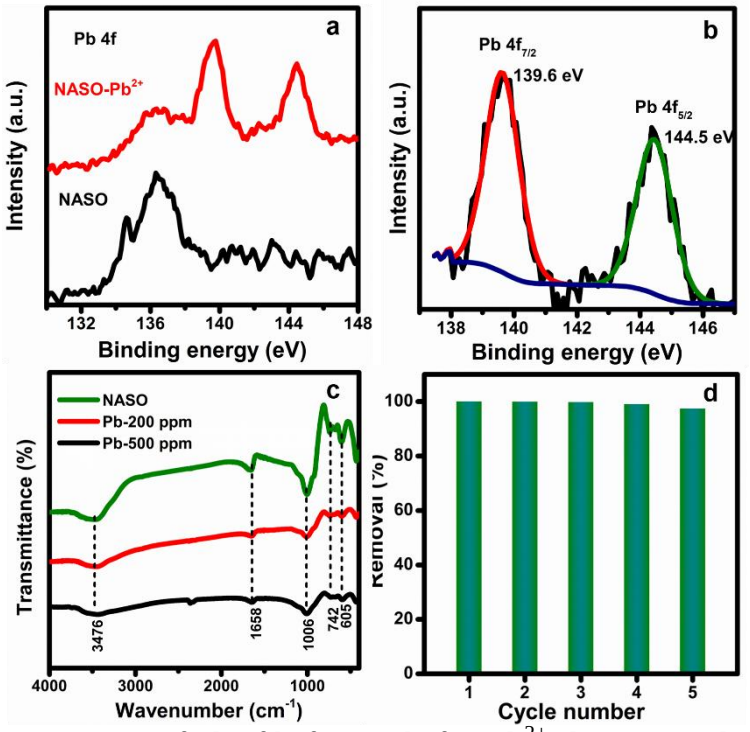

Figure 5. (a) XPS spectra of Pb 4f before and after Pb^{2+} absorption; (b) deconvoluted Pb 4f spectra of Pb^{2+} adsorbed sample; (c) FTIR spectra of the NASO before and after adsorption of Pb^{2+}; (d) Recycle performance of NASO towards Pb^{2+}.

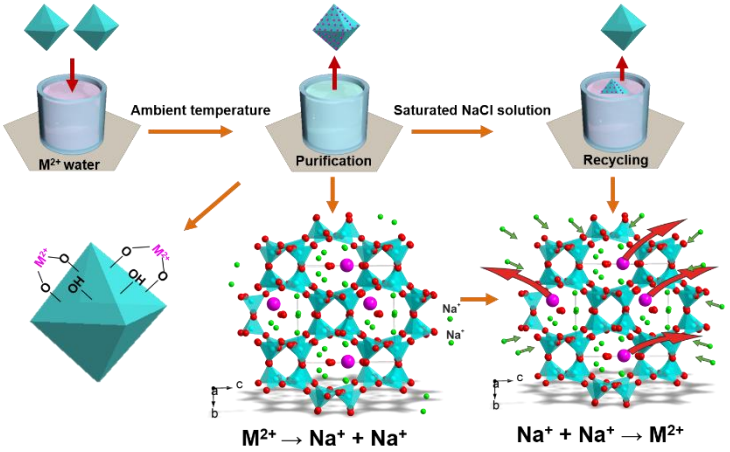

Figure 6. Schematic diagram of the adsorption and desorption of M^{2+} on NASO.

3.6 Comparison of the heavy metal removal efficiency of NASO with other zeolites

To the best of our knowledge, the Pb^{2+} uptake capacity of NASO was the top among zeolites reported for heavy metal adsorption (Table 5). Based on the analysis of absorption mechanism, we proposed the heavy metal uptake capacity of zeolites depended on: (1) cation exchange capacity (CEC), (2) pore size on the zeolite framework, (3) phase purify the OH groups of zeolites and (4) phase purity. So, we investigated the cation capacity, zeta potential and Pb^{2+} uptake capacity of commercial zeolite 4A and 13X for comparison displayed in Figure 7 and Table 6.

Table 5 The adsorption capacities of various zeolites for heavy metal ions

Absorbent	Metal	q_{max}(mg/g)	ref
Faujasite zeolite	Pb^{2+}	351	[39]
LTA zeolite	Pb^{2+}	514	
Zeolite A	Pb^{2+}	228	[40]
Synthetic clinoptilolite	Pb^{2+}	182	[31]
	Cd^{2+}	45	
Synthetic NASO	Pb^{2+}	649	this work
	Cd^{2+}	210	this work

Comparing with the pore size of three zeolites, it was apparent that all the unhydrated and hydrated M^{2+} ions could diffuse to the channels of zeolites, but the radius of hydrated ions was approximately the same as the channel size of zeolite 4A and they might exchange only with difficulty. Meanwhile, the lower zeta potential of NASO led to a greater uptake capacity of Pb^{2+} concerning zeolite 13X. Furthermore, the zeolite crystallinity and no impurity phase played important role in determining the heavy metal adsorption capacity. The NASO with much impurity phase prepared by using coal bottom ash revealed a low capacity of Pb^{2+} and Cd^{2+} (15.4 and 12.7 mg/g)[22]. Because some of the present cations for the ion exchange process were

components of impurities or they were located at inaccessible sites of the material structure, which were not suitable for ion exchange. On that account, the uptake capacities of heavy metal on the same type of zeolites were significant variation.

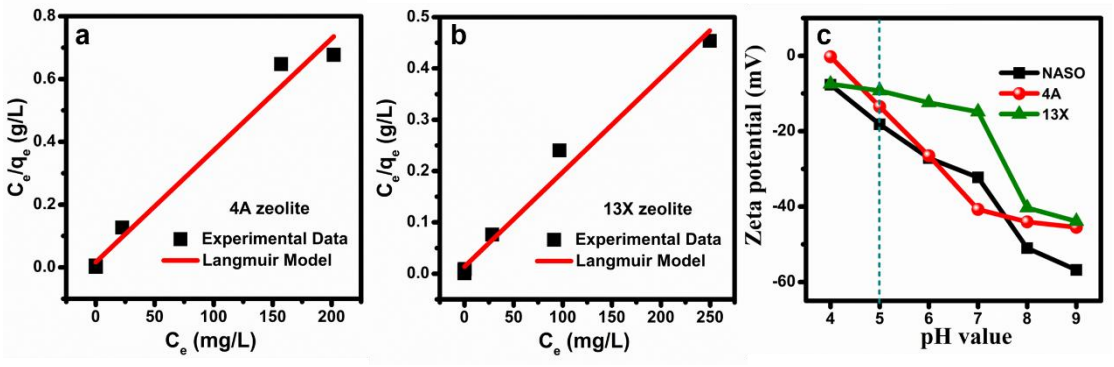

Figure 7. Sorption isotherms for adsorption of Pb^{2+} by (a) 4A and (b) 13X; (c) zeta potential measurement plots of zeolite 4A, 13X and NASO at different pH values.

Table 6 The adsorption capacities of various zeolites for heavy metal ions

Zeolite	Composition	Pore size (Å)	Theoretical CEC (mmol/g)	zeta potential pH = 5	Pb^{2+} q_{max} (mmol/g)
4A	$Na_{12}Al_{12}Si_{12}O_{48}\cdot 27H_2O$	4.2	5.4→2.7 Pb^{2+}	-13.48	1.37
13X	$Na_2Al_2Si_{2.46}O_{8.9}\cdot 6H_2O$	8	4.77→2.39 Pb^{2+}	-9.28	2.61
NASO	$Na_6Al_6Si_{10}O_{32}\cdot 12H_2O$	8.8	4.59→2.29 Pb^{2+}	-18.2	3.14

3.7 Competitive and effect of co-existing ions experiments

Moreover, complex competitive effects of different heavy metals in the real wastewater should be considered and the competitive experiments were conducted through mixing four ions with the same concentration. The results, listed in Table S5, made known that the selectivity order was Pb>Cu>Cd>Zn which was the same as the order of Pauling electronegativity. This indicated that NASO was very selective for ions with high electronegativity. Meanwhile, we also examined the influence of co-existing ions (100 ppm Na and 100 ppm Ca) on the absorption of single ion (10 ppm) and mixed ions (10 ppm). For single Cd^{2+}, Cu^{2+} or Zn^{2+} ion, the presence of Na and Ca caused a reduction in the adsorption capacity. Nevertheless, it had no effect on the adsorption of Pb^{2+} whatever it was single ion or mixed ion as shown in Table S6.

3.8 Reusable capacity of NASO

The reusability of absorption materials was an essential factor for practical application. Therefore, the desorption experiments were conducted to assess the regeneration feature of exhausted NASO via using a saturated NaCl solution as the eluting agent. The regeneration mechanism was ion exchange ($Pb^{2+}\rightarrow 2Na^{+}$) depicted

in Figure 6. For the absorption of 200 ppm Pb^{2+}, the Pb^{2+} removal rate of fresh adsorbents attained to 99.95%, and then a little loss of adsorption capacity (removal % = 97.4%) was observed after continuous four cycles in Figure 5(d), signifying that the NASO was repeatable and could be candidate for practical pollutant removal.

4. Conclusion

In conclusion, we found an unmodified and reusable zeolite $Na_6Al_6Si_{10}O_{32}\cdot 12H_2O$ for eradicating heavy metal accompanied by great capacity. The pure NASO with uniform octahedral shape was firstly prepared by regulating the ratio of Al/Si/NaOH/H_2O. The maximum capacities of Pb^{2+}, Cd^{2+}, Cu^{2+}, and Zn^{2+} were 649, 210, 90 and 88 mg/g on NASO which was better than other zeolites as we have known. The NASO could diminish Pb^{2+}concentration (4-130 ppm) down to < 1 ppb and the distribution coefficients (K_d) reached $\sim 10^8$ mL/g. Fast adsorption was observed that Pb^{2+} concentration (7.5 ppm) could be reduced to 0.6 ppb in 2 min. It also explained the relationship between adsorbent affinity and physicochemical properties of the heavy metals. The removal mechanism was accredited to the ion exchange and the hydroxyl groups on the surface of NASO. Based on the comparison of other zeolites, we proposed and verified the insights impacting the absorption capacity of zeolites. The presence of coexisting ions (Na and Ca) had no influence on the removal efficiency of Pb^{2+} and the removal rate of Pb^{2+} still kept 97.4% after five regeneration recycles. The NASO was thus a promising absorbent for practical pollutant treatment and industrialization.

Acknowledgements

This work was supported by the National Key R&D Program of China (Grant No. 2016YFB0901600); National Science Foundation of China (Grant Nos. 51402334 and 51502331); Science and Technology Commission of Shanghai (Grant No. 14520722000) and China Postdoctoral Science Foundation [Grant No. 8206300161].

Appendix A. Supplementary data

References

[1] S. Bolisetty, R. Mezzenga, Amyloid–carbon hybrid membranes for universal water purification, Nat. Nanotechnol., 11 (2016) 365.

[2] G.X. Zhao, J.X. Li, X.m. Ren, C.L. Chen, X.K. Wang, Few-layered graphene oxide nanosheets as superior sorbents for heavy metal ion pollution management, Environ. Sci. Technol., 45 (2011) 10454-10462.

[3] B.Y. Li, Y.M. Zhang, D.X. Ma, Z. Shi, S.Q. Ma, Mercury nano-trap for effective and efficient removal of mercury (II) from aqueous solution, Nat. Commun., 5 (2014) 5537.
[4] A. Jawed, V. Saxena, L.M. Pandey, Engineered nanomaterials and their surface functionalization for the removal of heavy metals: A review, Journal of Water Process Engineering, 33 (2020) 101009.
[5] X.D. Yang, Y.S. Wan, Y.L. Zheng, F. He, Z.B. Yu, J. Huang, H.L. Wang, Y.S. Ok, Y.S. Jiang, B. Gao, Surface functional groups of carbon-based adsorbents and their roles in the removal of heavy metals from aqueous solutions: a critical review, Chem. Eng. J., (2019) 608-621.
[6] R. Mukhopadhyay, D. Bhaduri, B. Sarkar, R. Rusmin, D.Y. Hou, R. Khanam, S. Sarkar, J.K. Biswas, M. Vithanage, A. Bhatnagar, Clay–polymer nanocomposites: Progress and challenges for use in sustainable water treatment, J. Hazard. Mater., 383 (2020) 121125.
[7] Y.C. Wang, Y. Gu, D.H. Xie, W.X. Qin, H.M. Zhang, G.Z. Wang, Y.X. Zhang, H.J. Zhao, A hierarchical hybrid monolith: MoS_4^{2-}-intercalated NiFe layered double hydroxide nanosheet arrays assembled on carbon foam for highly efficient heavy metal removal, J. Mater. Chem. A., 7 (2019) 12869-12881.
[8] L.J. Ma, Q. Wang, S.M. Islam, Y.C. Liu, S.L. Ma, M.G. Kanatzidis, Highly selective and efficient removal of heavy metals by layered double hydroxide intercalated with the MoS_4^{2-}ion, J. Am. Chem. Soc., 138 (2016) 2858-2866.
[9] W. Qiu, Y. Zheng, Removal of lead, copper, nickel, cobalt, and zinc from water by a cancrinite-type zeolite synthesized from fly ash, Chem. Eng. J., 145 (2009) 483-488.
[10] Y. Gossuin, A.-L. Hantson, Q.L. Vuong, Low resolution benchtop nuclear magnetic resonance for the follow-up of the removal of Cu^{2+} and Cr^{3+} from water by amberlite IR120 ion exchange resin, Journal of Water Process Engineering, 33 (2020) 101024.
[11] A. Sdiri, T. Higashi, T. Hatta, F. Jamoussi, N. Tase, Evaluating the adsorptive capacity of montmorillonitic and calcareous clays on the removal of several heavy metals in aqueous systems, Chem. Eng. J., 172 (2011) 37-46.
[12] M.K. Uddin, A review on the adsorption of heavy metals by clay minerals, with special focus on the past decade, Chem. Eng. J., 308 (2017) 438-462.
[13] R.Q. Wang, H.J. Chen, Y. Xiao, I. Hadar, K.J. Bu, X. Zhang, J. Pan, Y.H. Gu, Z.N. Guo, F.Q. Huang, $K_x[Bi_{4-x}Mn_xS_6]$, Design of a Highly Selective Ion Exchange

Material and Direct Gap 2D Semiconductor, J. Am. Chem. Soc., 141 (2019) 16903-16914.
[14] E. Rathore, P. Pal, K. Biswas, Layered metal chalcophosphate (K-MPS-1) for efficient, selective, and ppb level sequestration of Pb from water, J. Phys. Chem. C., 121 (2017) 7959-7966.
[15] D. Sarma, S.M. Islam, K. Subrahmanyam, M.G. Kanatzidis, Efficient and selective heavy metal sequestration from water by using layered sulfide $K_{2x}Sn_{4-x}S_{8-x}$ (x = 0.65-1; KTS-3), J. Mater. Chem. A., 4 (2016) 16597-16605.
[16] M.J. Manos, M.G. Kanatzidis, Sequestration of heavy metals from water with layered metal sulfides, Chem-Eur. J., 15 (2009) 4779-4784.
[17] K. Tabit, M. Waqif, L. Saâdi, Application of the Taguchi method to investigate the effects of experimental parameters in hydrothermal synthesis of Na-P1 zeolite from coal fly ash, Res. Chem. Intermed., (2019) 1-17.
[18] E. Olegario, C.M. Pelicano, J.C. Felizco, H. Mendoza, Thermal stability and heavy metal (As^{5+}, Cu^{2+}, Ni^{2+}, Pb^{2+} and Zn^{2+}) ions uptake of the natural zeolites from the Philippines, Mater. Res. Express, 6 (2019) 085204.
[19] K. Elwakeel, A. El-Bindary, E. Kouta, Retention of copper, cadmium and lead from water by Na-Y-Zeolite confined in methyl methacrylate shell, Journal of environmental chemical engineering, 5 (2017) 3698-3710.
[20] H. Shirzadi, A. Nezamzadeh Ejhieh, An efficient modified zeolite for simultaneous removal of Pb (II) and Hg (II) from aqueous solution, J. Mol. Liq., 230 (2017) 221-229.
[21] Y. Yurekliv, Determination of Adsorption Characteristics of Synthetic NaX Nanoparticles, J. Hazard. Mater., (2019) 120743.
[22] N.I. UM, G.C. HAN, K.S. You, J.W. Ahn, Immobilization of Pb, Cd and Cr by synthetic NaP1 zeolites from coal bottom ash treated by density separation, Resources Processing, 56 (2009) 130-137.
[23] D.D. Do, Adsorption analysis: equilibria and kinetics, Imperial college press London, 1998.
[24] D.M. Jiang, Y.H. Yang, C.T. Huang, M.Y. Huang, J.J. Chen, T.D. Rao, X.Y. Ran, Removal of the heavy metal ion nickel (II) via an adsorption method using flower globular magnesium hydroxide, J. Hazard. Mater., 373 (2019) 131-140.
[25] N. Arancibia Miranda, S.E. Baltazar, A. García, D. Muñoz Lira, P. Sepúlveda, M.A. Rubio, D. Altbir, Nanoscale zero valent supported by zeolite and

montmorillonite: template effect of the removal of lead ion from an aqueous solution, J. Hazard. Mater., 301 (2016) 371-380.
[26] C.-H. Weng, Modeling Pb (II) adsorption onto sandy loam soil, J. colloid. inter. sci., 272 (2004) 262-270.
[27] H. Aydın, Y. Bulut, Ç. Yerlikaya, Removal of copper (II) from aqueous solution by adsorption onto low-cost adsorbents, J. Environ. Manage., 87 (2008) 37-45.
[28] S.B. Yang, J. Hu, C.L. Chen, D.D. Shao, X.K. Wang, Mutual effects of Pb (II) and humic acid adsorption on multiwalled carbon nanotubes/polyacrylamide composites from aqueous solutions, Environ. Sci. Technol., 45 (2011) 3621-3627.
[29] J. Perić, M. Trgo, N.V. Medvidović, Removal of zinc, copper and lead by natural zeolite-a comparison of adsorption isotherms, Chem. Eng. J., 38 (2004) 1893-1899.
[30] Y. Shin, G.E. Fryxell, W. Um, K. Parker, S.V. Mattigod, R. Skaggs, Sulfur- functionalized mesoporous carbon, Adv. Funct. Mater., 17 (2007) 2897-2901.
[31] Y.R. Li, P. Bai, Y. Yan, W.F. Yan, W. Shi, R.R. Xu, Removal of Zn^{2+}, Pb^{2+}, Cd^{2+}, and Cu^{2+} from aqueous solution by synthetic clinoptilolite, Micropor. Mesopor. Mat., 273 (2019) 203-211.
[32] A. Hawari, M. Khraisheh, M.A. Al-Ghouti, Characteristics of olive mill solid residue and its application in remediation of Pb^{2+}, Cu^{2+} and Ni^{2+} from aqueous solution: Mechanistic study, Chem. Eng. J., 251 (2014) 329-336.
[33] F. Pagnanelli, A. Esposito, L. Toro, F. Veglio, Metal speciation and pH effect on Pb, Cu, Zn and Cd biosorption onto Sphaerotilus natans: Langmuir-type empirical model, Water Res., 37 (2003) 627-633.
[34] E. Nightingale Jr, Phenomenological theory of ion solvation. Effective radii of hydrated ions, J. Phys. Chem. C., 63 (1959) 1381-1387.
[35] M. Uudsemaa, T. Tamm, Calculation of hydration enthalpies of aqueous transition metal cations using two coordination shells and central ion substitution, Chem. Phys. Lett., 400 (2004) 54-58.
[36] W.W. Rudolph, C.C. Pye, Zinc (II) hydration in aqueous solution. A Raman spectroscopic investigation and an ab-initio molecular orbital study, Phys. Chem. Chem. Phys., 1 (1999) 4583-4593.
[37] K. Hui, C.Y.H. Chao, S. Kot, Removal of mixed heavy metal ions in wastewater by zeolite 4A and residual products from recycled coal fly ash, J. Hazard. Mater., 127 (2005) 89-101.
[38] D. Nibou, S. Khemaissia, S. Amokrane, M. Barkat, S. Chegrouche, A. Mellah,

Removal of UO_2^{2+} onto synthetic NaA zeolite. Characterization, equilibrium and kinetic studies, Chem. Eng. J., 172 (2011) 296-305.
[39] M. Hong, L.Y. Yu, Y.D. Wang, J. Zhang, Z.W. Chen, L. Dong, Q.j. Zan, R.L. Li, Heavy metal adsorption with zeolites: The role of hierarchical pore architecture, Chem. Eng. J., 359 (2019) 363-372.
[40] Q.P. Meng, H. Chen, J.Z. Lin, Z. Lin, J.L. Sun, Zeolite A synthesized from alkaline assisted pre-activated halloysite for efficient heavy metal removal in polluted river water and industrial wastewater, Journal of environmental sciences, 56 (2017) 254-262.

Declaration of interest statement

The authors declare that they have no competing financial interests or personal relationships that could have appeared to influence the work reported in the paper.

Graphical abstract

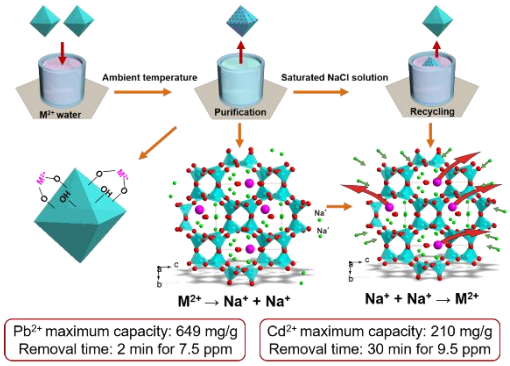

Herein, we firstly synthesized the octahedral zeolite $Na_6Al_6Si_{10}O_{32}\cdot 12H_2O$ without modification for eradicating heavy metal ions, proven great absorption capacity. Rapid adsorption and stable recycling performance made the zeolite to be promising for practical water purification and industrialization.

Highlights

- The synthetic NASO zeolite without modification for eradicating heavy metal.
- The great absorption capacities for Pb and Cd are 649 and 210 mg/g.
- Rapid purification for Pb wastewater to drinkable level is in 2 min.
- Adsorption involves both ion exchange reaction and electrostatic interaction.
- Easy preparation and stable recycling performance let it for practical application.

Supplementary Material

Click here to download Supplementary Material: Supplementary material.docx